FINAL TECHNICAL REPORT

LIGHT REFLECTANCE, TRANSMITTANCE, AND UTILIZATION WITHIN A VEGETATIVE CANOPY

by

E. W. LeMaster, Department of Physical Science
J. E. Chance, Department of Mathematics
Pan American University
Edinburg, Texas 78539

prepared for

NATIONAL AERONAUTICS AND SPACE ADMINISTRATION
Headquarters, Washington, D. C. 20546

April, 1980

Funding 1 October, 1978 to 30 September, 1979

Contract NSG 9033 Supplement 3

INTRODUCTION

The research carried out under grant NSG-9033-3 was directed toward the following objectives:

1. Construct and test equipment and collect field data to verify the light absorption model (LAM) developed from the differential equations Suits [1] derived in his bidirectional reflectance model.

2. Use the Suits model of reflectance and a suitable atmospheric model to predict the Landsat-2 Multispectral Scanner (MSS) digital counts.

This report is divided into two main parts. The first is a description of the equipment developed from a basic design of Norman, Thurtell, and Tanner [2] for the measurement of light absorption within the canopy. The last part is a detailed description of the method developed to extend ground-based bidirectional reflectance measurements up through a standard atmosphere, through the filter and gain factors of the MSS, and express the results as MSS digital counts in the four Landsat-2 channels. Further use of the method to express Suits model calculations as Landsat-2 digital counts is discussed.

The rationale for the project is to strive for ways to utilize the predictive power of the Suits model. The first objective that concerns the light absorption model is our effort to both accurately describe the light interception by a vegetative canopy and to attempt to measure this important

quantity from the reflected radiation. Once the method is verified as both possible and accurate, then application to the real field situation may not be possible because of soil background variability or variability of the atmosphere. Application of the second method of extending ground-based or model-based bidirectional reflectance to satellite responses will provide a valuable tool in establishing cause and effect. Many questions can be answered through such a capability such as: What is the minimum detectable vegetation on a given soil? Can a change in leaf slope be detected from satellite? How do the digital counts change as a fixed amount of vegetation (Leaf Area Index) is redistributed from 100% ground cover to, say, 30% ground cover?

Certainly all the questions one asks of a model will not be answered quantitatively correctly, but certainly the answer can yield some measure of understanding of the trends expected.

CHAPTER I

LIGHT MEASURING STICK

Light interception measurements in plant canopies are difficult to make because of the strong variation in light intensities at a given level. The approach that has been used by many agronomists is a radiometer device mounted on a horizontal track such that a continuous measurement across several rows could be integrated to give a mean value for a fixed sun angle. The limitations of this method were (a) lack of portability and (b) expense. The solution we have devised has solved both problems. The possible trade-off is perhaps a less representative average value for the light intensity at a given level in the canopy when made from a single reading. Some possible solutions to this limitation will be suggested after the device is described.

Light Stick Design

During the time we were working on the light absorption model, the question was frequently asked, "how can we verify this calculation?" Dr. Ed Kanemasu mentioned such a device that could be easily constructed from readily available and inexpensive components. He referred us to the work of Norman, Thurtell and Tanner[2] as a source of specific filters that could be used on the device. The light detector is a J4800 silicon photovoltaic cell manufactured by GC Electronics, Division of Hydrometals, Inc., Rockford, Illinois 61100, with a spectral sensitivity in the range 400-1200 nm. The cost was about $4.00 each from a local electronics supply house. A light diffuser as shown in the diagram was needed

Cosine Response Graph

— Ideal Cosine Response
⊙ Actual Cosine Response
For Opalized Glass

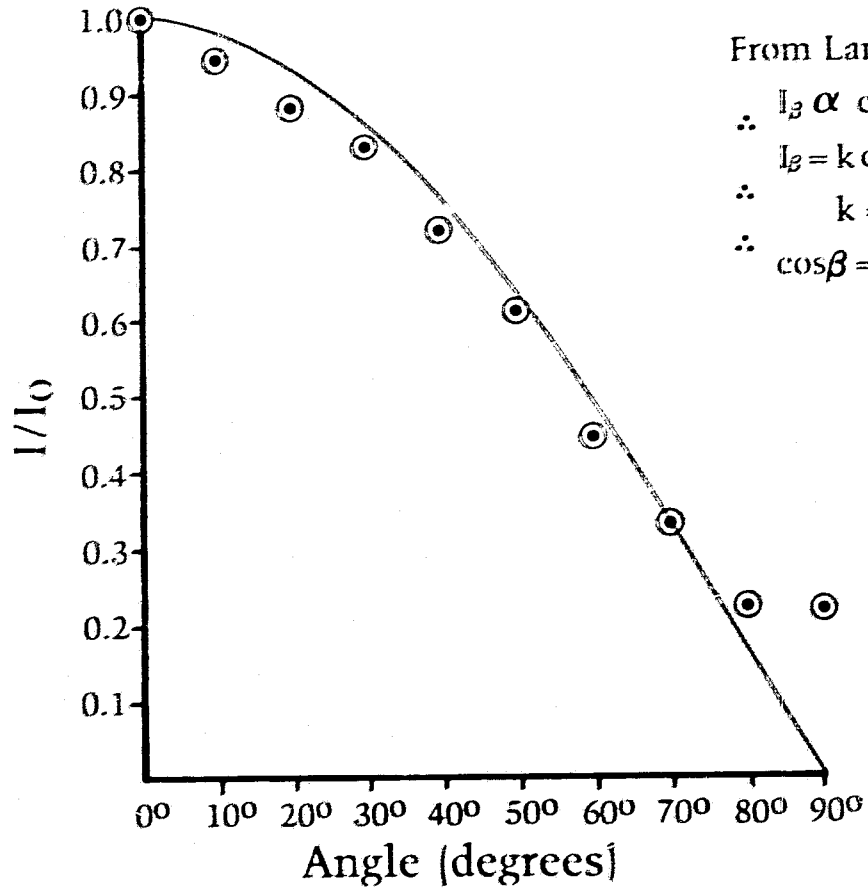

From Lamberts Law

$\therefore I_\beta \alpha \cos\beta$

$I_\beta = k\cos\beta$ where $k = I_\beta/\cos\beta$

$\therefore k = I_\beta$ when $\beta = 0^\circ$

$\therefore \cos\beta = \frac{I_\beta}{I_n}$

FIGURE 1

to insure that the photocell could accept light equally from all angles. The array with diffuser viewing a collimated light source should show an ideal cosine response.

Diffuser materials were tested extensively for the ideal cosine response (Lambert's Law). We tested:

a) 1 mm thick teflon

b) 4 mm thick teflon

c) 3 mm thick plastic foam packing material

d) white paper (thin)

e) opalized white glass, 6 mm thick

f) frosted glass

g) sandwich of teflon and glass

h) thin glass plates

i) thin clear plastic

j) sanded plastic.

Good cosine response was obtained from both the white paper and the opalized white glass. The opalized glass response is shown in Fig. 1. The glass was chosen because it had a larger transmittance in the visible spectrum than the white paper. Kerr, Thurtell, and Tanner[3] point out the advantage of using a thick material for a diffuser because the edges pick up light at large angles of incidence. Opalized glass was used for these reasons.

The fact that this diffusing material was quite thick may have helped the acceptance of radiation at large angles because of the radiation entering the edges. The white opalized glass was obtained from a local supplier of plate glass. They cut it into small squares that would just fit the

clear plastic case in which the photocells were shipped. The photocells were 18 mm x 18 mm so the glass was about 20 mm on a side. The glass squares were then connected to the clear plastic with clear epoxy. The gelatin filters were ordered from a Kodak photo products dealer, CC-20M Wratten and Wratten 89-B. Since measurements in the photosynthetically active region (PAR) are usually desired, the filters were used to obtain a sensitivity from 500-700 nm. (See Fig. 2.)

The silicon cell must have its ir response filtered to accomplish a reading of the PAR. Selenium cells have been[4] used because they don't respons to ir, but they have many undesirable effects, i.e., fatigue in high illumination, insensitivity at low light levels, and large temperature sensitivity. A further purpose of the filters is to tailor the response so that a quantum response is obtained such that an energy flux is obtained from the cell reading. (See Fig. 3 .)

Each silicon cell was checked and they were grouped by their response to a constant light source. The small differences were presumably due to surface imperfections or variations in doping. The 24 cells tested were divided into two groups and the highest 2 and lowest 2 cells were eliminated; the remaining differed by only a few percent in their response to a fixed source of light. The cells were partially masked with vinyl electrical tape to give less than 1% variation from cell to cell.

The plastic units in which the photocells, filters, and diffuser were located were then connected on 10 cm centers along a slender aluminum strip about 130 cm long to allow a

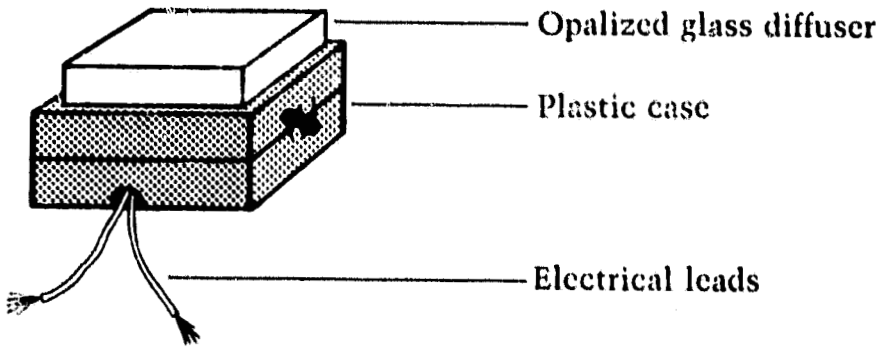

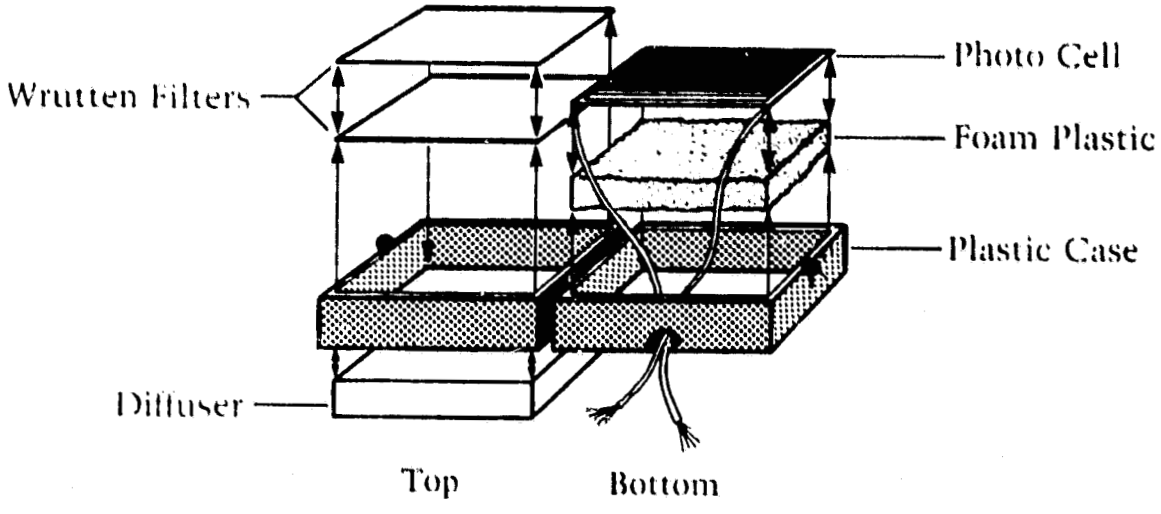

FIGURE 2

% Transmittance vs. Wavelength Graph

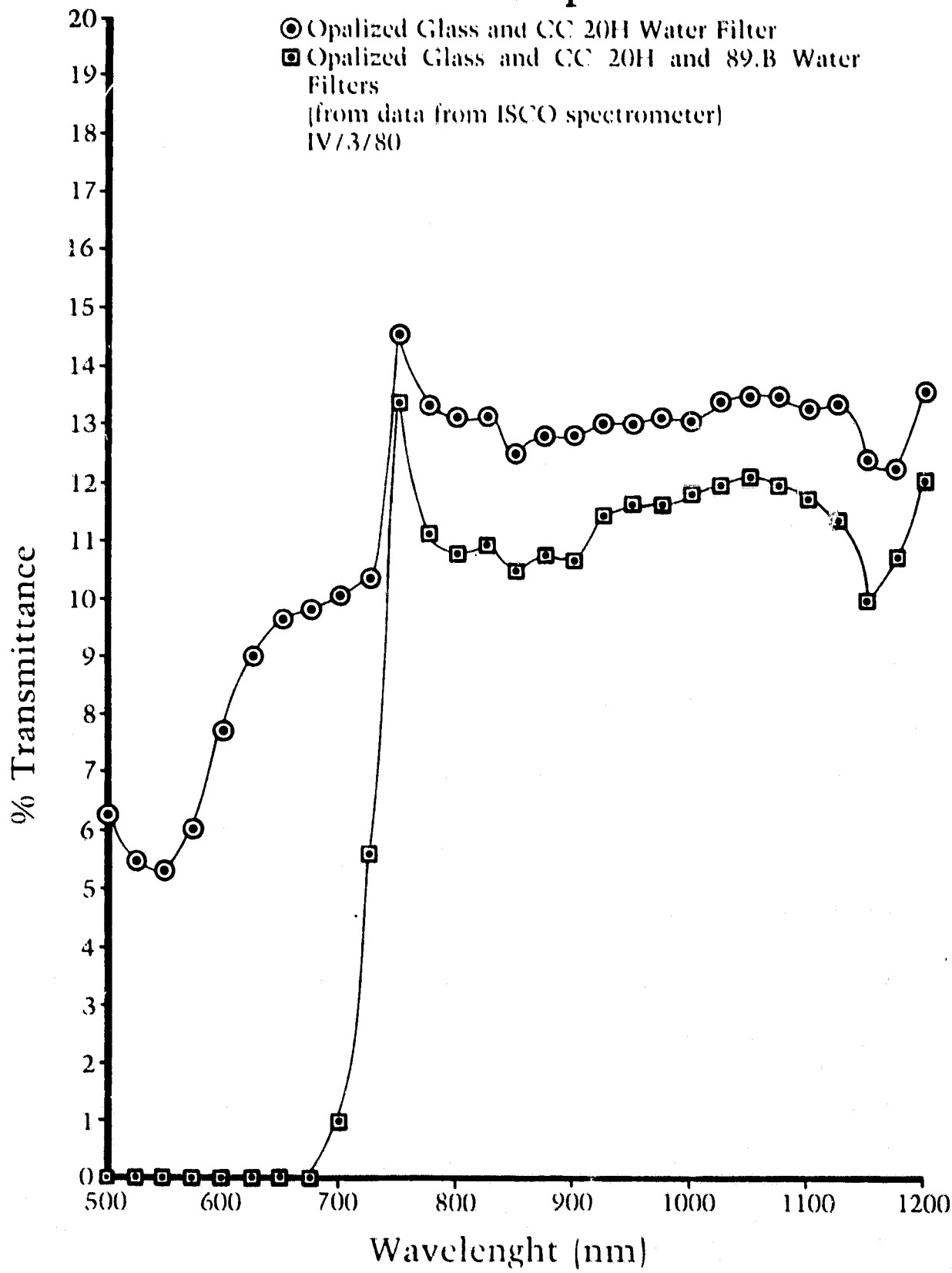

FIGURE 3

short distance at one end for a hand grip. The cells were wired in parallel and connected to a double throw toggle switch so that the short circuit current could be read through a 500mA ammeter. (See Fig. 4.)

Use of the Light Stick

The instrument was tested for about 15-20 hours in a dense cotton field near McAllen, Texas. Two problems surfaced during the testing. The first was the mechanical connection of the wire between the ammeter and the light stick. This wire was about 3m long to allow a second person to hold the meter and record readings while the operator placed the stick at various levels. A very flexible wire was used to replace the original, stiff wire. The second problem was that a plastic case opened up upon contact with a cotton stalk and the filters blew away in the wind. The problem was not solved but care was exercised in the future to prevent a recurrence of the problem. Spare filters were always carried to the field with the instrument.

Use of the instrument was as follows: the stick was placed horizontally above the level of the crop in with the visible- and ir-sensitive (VIR) cells looking vertically upward and the ir-sensitive cells looking downward. The switch is operated by the person holding the meter and recording data. The stick is then rotated to give a reading from downward-looking VIR cells and upward-looking ir cells. The incoming PAR at the top of the canopy is obtained by subtracting the ir (upward-looking) from the VIR (upward-looking). The same procedure for downward-looking readings

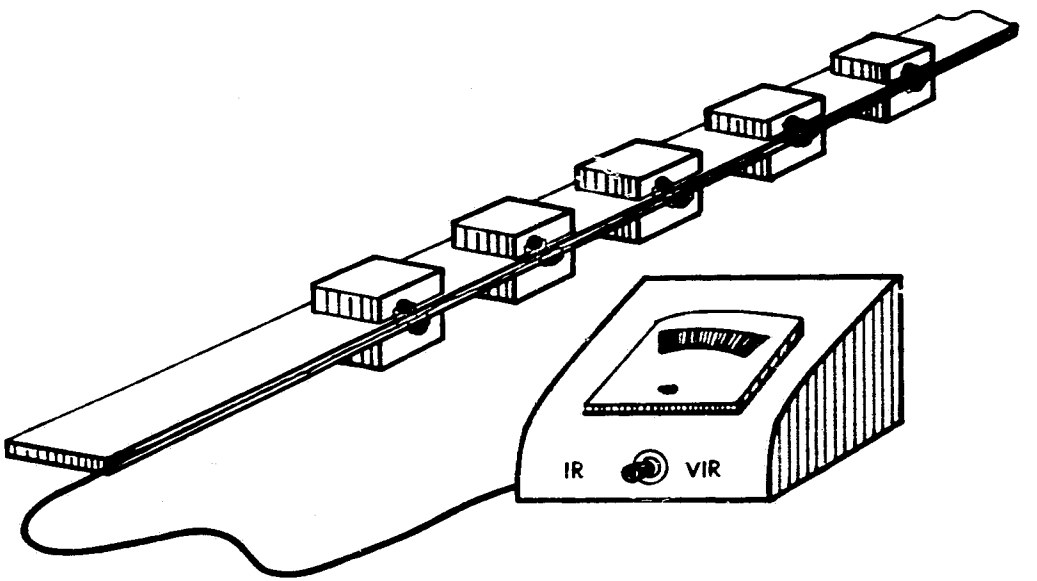

Light Stick

FIGURE 4

yields the PAR leaving the canopy and thus the ratio gives the reflectance over the PAR spectrum. Likewise the ir reflectance can be calculated.

The light abosrbed in any layer can be similarly measured by the incoming, reflected, and transmitted radiation. In any layer the absorbed energy is the difference between the incoming and outgoing. The percent can be found by dividing by the incoming. One then adds the downwelling radiation at the top and the upwelling radiation at the bottom of the layer to give the total coming in. The outgoing is the upwelling at the top plus the downwelling at the bottom. Any horizontal layer can be measured in this manner.

REFERENCES

1. Suits, G. H., Remote Sens. Environ. 2, 117 (1972).

2. Norman, J. M., C. B. Tanner, and G. W. Thurtell, Agron. J. 61, 840 (1969).

3. Kerr, J. P., G. W. Thurtell, and C. B. Tanner, J. Appl. Meteor. 6, 688 (1967).

4. Muchow, R. C., and G. L. Kerven, Agric. Meteor. 18, 187 (1977).

CHAPTER II

CROP IDENTIFICATION AND LEAF AREA INDEX CALCULATIONS WITH LANDSAT MULTITEMPORAL DATA

Introduction

LeMaster and Chance [1] have shown that the Suits Model for vegetative canopy reflectance predicts a simplified functional relationship for canopy reflectance as a function of

λ - wavelength (nm)

n - leaf area index (LAI)

m_1 - air mass between sun and crop canopy

m_2 - air mass between sensor and crop canopy.

This relationship is

$$R(\lambda,n,m_1,m_2) = R(\lambda,0,m_1,m_2)e^{-K(\lambda)n} + R(\lambda,\infty,m_1,m_2)\left[1 - e^{-K(\lambda)n}\right] \qquad (1)$$

where

$K(\lambda)$ is the canopy extinction coefficient and $R(\lambda,n,m_1,m_2)$ is the crop target reflectance which varies from that of bare soil $R(\lambda,0,m_1,m_2)$ (LAI-0) to infinite crop reflectance $R(\lambda,\infty,m_1,m_2)$ (LAI large). Canopy infinite reflectance is exhibited whenever the addition of more leaves and vegetative components to the canopy by growth fails to change the canopy reflectance [2]. Infinite reflectance has been observed experimentally for leaves stacked over the port of a spectrophotometer [2], and infinite reflectance values have also been published for wheat crops [3].

Experimental tests [4] have shown that infinite crop reflectance is attained for crops at all wavelengths whenever the crop LAI is in excess of 8. Figure 1 is a graph of the spectral infinite reflectance curves for sugarcane and wheat with LAI in excess of 8 from 500-1100 nm. The sugarcane reflectance data was taken from unpublished data of Dr. Ross Leamer [5] and the wheat reflectance data appears in [6]. It should be noted that only minor differences in the reflectance of these two crops occur in the visible region, while significant differences occur in the infrared region. Such differences similarly occur in Landsat data for channels 3 and 4, as will be shown later in this paper and can be used for discrimination purposes. The bare soil spectral reflectance curve shown in Figure 1 illustrates the fact that poor contrast exists between soil and vegetation in the visible channels, while a good contrast exists for the infrared channels. Further, since canopies are more reflective than bare soil in the infrared, digital counts in Landsat multispectral scanner (MSS) channels 3 and 4 should increase as the crops increase their LAI. On the other hand, since canopies are less reflective than bare soil in MSS channel 2, digital counts should decrease as crops increase their LAI.

Equation (1) can be implemented by knowing the canopy extinction coefficients $K(\lambda)$. Norman [7] has collected extinction coefficients measured by other authors for several crops and concluded that variability exists in these measurements. However, this author has used experimental field reflectance spectra for grain sorghum to determine that the extinction coefficient remains constant within the 500-700 nm region, and changes at about 700 nm to a new value, but remains constant at that value from 700-1100 nm. That is,

$$K(\lambda) = K_V, \quad 500 \leq \lambda \leq 700$$

$$= K_I, \quad 700 < \lambda \leq 1100.$$

Such behavior of the extinction coefficient is probably characteristic of all crops, with the constants K_V and K_I changing for different crops.

The purposes of this paper are to use equation (1) to explain Landsat data taken at different times during the growing season of commercial cultivars. Equations are given to convert ground-based crop reflectance measurements into Landsat digital counts for a standard atmosphere, and finally methods are developed for the use of Landsat data for crop identification and to determine crop LAI.

Formulas for the Conversion of Ground-Based Reflectance Measurements to Landsat Digital Counts

It is not the author's purpose to develop a detailed atmospheric transfer model in this paper. Models have been developed that consider a wide variety of input parameters. A notable example is the atmospheric model developed by Turner [8].

A model can be derived by considering sequentially the modifications of a light beam entering the atmosphere and traveling downward to a vegetative canopy, being reflected from the canopy, traveling upward through the atmosphere to Landsat, and finally being converted by the Landsat ground system to digital counts. The number of digital counts in channel i, Ch(i) for i=1,2,3,4 is

$$Ch(i) = \frac{1}{\pi A(i)} \int_{\alpha_{i-1}}^{\alpha_i} E(\lambda, m_1)\ R(\lambda, n, m_1, m_2)\ D(\lambda, l)\ K(\lambda, i)\, d\lambda + \frac{1}{A(i)} \int_{\alpha_{i-1}}^{\alpha_i} L_p(\lambda)\, d\lambda - \frac{B(i)}{A(i)} \tag{2}$$

where

(i) $E(\lambda,m_1)$ is the solar spectral radiant flux for air mass m_1 (watts $cm^{-2}nm^{-1}$). The data used came from Elterman [9], being derived for the transmission of a clear standard atmosphere using a Rayleigh atmosphere combined with aerosol components and 35 cm total ozone content. This transmission data multiplied by the data collected by Thekaekara [10] for solar spectral radiant flux with zero air mass gave the required results.

(ii) $D(\lambda,1)$ is the transmittance of the atmosphere through a vertical path. Again, this data was found in Elterman.

(iii) $K(\lambda,i)$ is the relative response of channel i in the Landsat system to wavelength λ. These response functions were found in Henderson, Thomas, and Nalepka [11] for Landsat-1.

(iv) $A(i),B(i)$ are Landsat calibration constants for channel i as given by Richardson [12]. The subsequent equations that appear in this section of the paper were derived for Landsat-1 in its early stages, but a transformation is given that will convert these results to later Landsat systems.

(v) $L_p(\lambda)$ is the atmospheric path radiance, the most difficult quantity to estimate. Estimates of these were obtained from data taken by Ahern [13] from Landsat using clear lakes as dark background. For use in equation (2), Ahern's measurements were averaged over 6 reporting dates given with air masses and condition of the atmosphere unknown. An analysis of the effect of path radiance with varying air masses was done by Richardson [14] for a clear standard atmosphere using the atmospheric model of Turner. This analysis indicated that for air masses in excess of 1.2, digital counts varied less than 5 counts in channel 3 and 1 count in

channel 4.

(vi) α_{i-1}, α_i are the lower and upper limits of wavelengths (nm) for radiant energy detected in channel i of Landsat.

$\alpha_0 = 500$, $\alpha_1 = 600$, $\alpha_2 = 700$, $\alpha_3 = 800$, $\alpha_4 = 1100$.

The digital counts for channels 1, 2, and 3 vary from 0 to 127 and channel 4 varies from 0 to 63.

Equation (2) was evaluated using the trapezoidal rule for numerical integration at 50 nm step sizes over the respective channels. This step size was chosen to confirm to previously measured ground-based reflectance measurements taken by LeMaster and Chance [15] for wheat, grain sorghum, and cotton. The results are as follows: if $R(\lambda)$ denotes the crop reflectance at wavelength λ, and 0 is the solar zenith angle,

$$\begin{aligned}
Ch(1) &= 48.6 \exp(-.370\text{Sec}0)R(500) + 100 \exp(-.331\text{Sec}0)R(550) \\
&\quad + 54.4 \exp(-.305\text{Sec}0)R(600) + 16 \\
Ch(2) &= 67.6 \exp(-.305\text{Sec}0)R(600) + 127.6 \exp(-.252\text{Sec}0)R(650) \\
&\quad + 51.1 \exp(-.217\text{Sec}0)R(700) + 11 \\
Ch(3) &= 66.8 \exp(-.217\text{Sec}0)R(700) + 87.5 \exp(-.200\text{Sec}0)R(750) \\
&\quad + 39.4 \exp(-.187\text{Sec}0)R(800) + 11 \\
Ch(4) &= 10.2 \exp(-.187\text{Sec}0)R(800) + 18.3 \exp(-.177\text{Sec}0)R(850) \\
&\quad + 13.2 \exp(-.166\text{Sec}0)R(900) + 9.0 \exp(-.159\text{Sec}0)R(950) \\
&\quad + 5.4 \exp(-.151\text{Sec}0)R(1000) + 2.6 \exp(-.148\text{Sec}0)R(1050) \\
&\quad + 3
\end{aligned}$$

These formulas should not be used for solar zenith angles (0) in excess of 72°, as correction for atmospheric refraction of light must be made [16].

Equations (3) apply only to Landsat-1 from 1-22-75 to 7-15-75, but can be corrected to model Landsat data on other dates by

adjustment of the calibration constants. If Ch2(i) is the digital count in channel i of Landsat on one of the other dates given in Table 1, then one uses equations (3) to find Ch(i) and

$$Ch2(i) = Ch(i) \cdot C(i) - D(i).$$

The C(i) and D(i) are constants listed in Table 1 as adapted from the data of Richardson [12] for dates from 1-22-75 to at least 1977. For use on later Landsat data, it should be determined whether subsequent changes in the calibration constants have been made.

Figure 2 is a plot of channel 3 against channel 4 for Landsat-1 using equations (3). The data taken came from Condit [17] in the form of the spectral reflectance curves for American soils taken from 14 sites, and appears as circled dots. This data reproduces the Kauth soils line [18], with low reflective soils appearing as data points in the lower left side of the graph and high reflective soils appearing in data in the upper right side of the graph. The data plotted in Figure 2 as crosses appears in Richardson [19] taken from Landsat-1 digital counts for high and low reflecting bare soils in Hidalgo and Willacy Counties, Texas.

Figure 3 is another plot of channel 3 versus channel 4 Landsat digital counts using grain sorghum multitemporal spectral reflectance data collected by LeMaster and Chance [20] as ground-based measurements. The circled dots are simulated digital counts using equations (3) with a sun zenith angle of 28°. It is of interest to observe that the simulated data initiates at a point on the Kauth soils line and progresses upward during the growing season along a near straight line with increasing LAI. During the observation period this grain sorghum had an LAI that increased from 0 to 3.

This data compares favorably with data collected by Richardson

[21] from Landsat-1 for grain sorghum fields in the Lower Rio Grande Valley of Texas. These data, appearing as crosses, were taken from a single frame of Landsat data having a sun zenith angle of 28°. The ground truth was collected for these same fields, with reported LAI ranging from 3 to 8.5. Again, the data rises along what appears to be the same straight line as the simulated Landsat data with increasing LAI and joins the line at an LAI of 3. This figure suggests that an appropriate scaling of the line along which the data points increase would yield information on crop LAI. Such a result is established later in the paper.

Figure 4 is a plot of channel 3 versus channel 4 digital counts for Landsat-1 wheat data. The circled dots represent simulated Landsat-1 counts using equations (3) with multitemporal spectral reflectance data for Penjamo wheat collected by LeMaster and Chance [6]. The data points again rise from the Kauth soils line with increasing LAI along a near straight line (r^2=.97) reaching a maximum displacement for the maximum LAI of 4.09 at the flowering stage. Past the flowering stage to the grain filling stage the leaves lose their green color and LAI decreases resulting in a decrease in canopy reflectance in the infrared. The corresponding Landsat digital counts decrease in both channels 3 and 4, but the points remain on the same line as formed when the LAI was increasing. This suggests that leaf water and chlorophyll content changes that occur in a wheat canopy as it matures affects channel 3 and 4 in an equal manner. Further, it suggests that growth stages for wheat cannot be determined solely by plots of channel 3 versus channel 4.

The dots that appear in Figure 4 are simulated Landsat-1 digital counts using spectral reflectance data in equations (3). The data was collected by Project LACIE for Williston, North Dakota, in 1976 [3]. The data points rise from the Kauth soils line along a straight line with increasing LAI.

The crosses that appear in Figure 4 are actual Landsat-1 multitemporal digital counts collected by Kanemasu [22] for wheat grown in Riley County, Kansas. Ground truth was collected for this site, and as predicted by the simulation, the data points rise with increasing LAI along a near straight line (r^2=.95) reaching a maximum displacement at the maximum LAI of 3.49. The Landsat data points appear to be laterally displaced from the simulation points, but this can be explained by differences in soil reflectance between Riley County, Kansas, Hidalgo County, Texas, and Williston, North Dakota. That is, the data sets emerge from different points along the Kauth soils line. The regression lines are plotted for each data set and it can be seen that for low LAI the lines are divergent because not much of the vegetative canopy covers the soil, and the two different soils have different reflectances. As the LAI increases, and the data points rise along each of the respective lines, the lines converge. The dissimilar soils are being covered by vegetation whose reflectances are similar. It is of interest to note that the lines cross at the point (65,32), implying that for very large LAI and complete ground coverage, wheat, regardless of the geographic area, looks similar in channels 3 and 4 of Landsat. An important idea can thus be extracted from Figure 4: regardless of geographic location, wheat multitemporal data in Landsat channels 3 and 4 produce a linear pattern that

progresses toward the neighborhood of the point (65,32). In fact, the regression lines are close to being parallel, so that all lines are within one digital count of equality from (53,22) onward. Other Landsat data are needed especially for wheat grown on a highly reflective soil to sharpen the estimate on this neighborhood. On the basis of this evidence, it appears that infinite reflectance spectra is an important parameter that should be collected for a crop. If one applies equation (3) to the infinite reflectance curves for sugarcane and wheat shown in Figure 1 using a 28° solar zenith angle the following is obtained: sugarcane channel 3, 81, channel 4, 34; wheat channel 3, 56, channel 4, 28. Thus the wheat infinite reflectance point falls within the neighborhood shown in Figure 4 and more importantly, the infinite points for sugarcane and wheat are distinct. Thus multitemporal sugarcane data points emerge from the Kauth soils line in a different direction than wheat data points.

Reflectance spectra were obtained for other crops having a large LAI and converted into Landsat-1 digital counts using equations (3) and the results are found in Table 2. Figure 5 is a plot of these points and the idealized multitemporal traces made by channel 3 versus channel 4 Landsat digital counts for each of the four crops grown in eastern Hidalgo County, Texas. It is of interest to note that the points are separated as to crop type with a wide divergence between grain sorghum and sugarcane and a narrow divergence between wheat and corn. Whether such differences can be observed with actual Landsat data should be tested with available data sources. Figure 5 seems reasonable, since it implies that in the early stages of growth with low LAI mostly soil

is showing, and each of the lines is close to the soil point so that crop discrimination is difficult, As the crops increase their LAI, differences in their digital counts appear more apparent as mostly vegetation is showing and at this stage crop discrimination should be easier. The differences in digital count for different crops is not easy to explain. Gausman, et al, [23] have measured single leaf reflectances for twenty crops, and their results indicate very little difference between individual leaves. Possible differences between crops in the near infrared lie in such characteristic species architecture of field grown plantings as leaf slope, leaf size and shape, and plant height.

Multitemporal Behavior of Landsat Data

To model the multitemporal behavior of Landsat data, substitute equation (1) into (2). After some simplification

$$Ch(i) = S(i)e^{-K_V n} + I(i)\left[1-e^{-K_V n}\right] - \frac{B(i)}{A(i)} + L(i) \qquad (4)$$

for $i = 1,2$

$$Ch(i) = S(i)e^{-K_I n} + I(i)\left[1-e^{-K_I n}\right] - \frac{B(i)}{A(i)} + L(i) \qquad (5)$$

for $i = 3,4,$

where

$$S(i) = \frac{1}{\pi A(i)} \int_{\alpha_{i-1}}^{\alpha_i} E(\lambda,m_1)D(\lambda,1)R(\lambda,0,m_1,m_2)K(\lambda,i)d\lambda$$

$$I(i) = \frac{1}{\pi A(i)} \int_{\alpha_{i-1}}^{\alpha_i} E(\lambda,m_1)D(\lambda,1)R(\lambda,\infty,m_1,m_2)K(\lambda,i)d\lambda$$

$$L(i) = \frac{1}{A(i)} \int_{\alpha_{i-1}}^{\alpha_i} Lp(\lambda)d\lambda.$$

S(i) is the term that measures the effects of bare soil radiance on Landsat data, I(i) is the term that measures the effects of infinite crop radiance on Landsat data, and L(i) measures the effects of atmospheric path radiance on Landsat data. In what follows it will be assumed that S(i), I(i), and L(i) remain constant for every data acquisition date of Landsat. Such will never be the case for any real situation, however, since soil reflectance changes with change in soil moisture, the quality of the atmosphere varies from day to day, and the solar air mass varies slightly from one acquisition date to another due to solar declination.

Using the above assumptions, solving equations (4) for $e^{-K_V n}$ and equating like terms yields

$$\frac{Ch(1) - I(1) + \frac{B(1)}{A(1)} - L(1)}{S(1) - I(1)} = \frac{Ch(2) - I(2) + \frac{B(2)}{A(2)} - L(2)}{S(2) - I(2)} . \quad (6)$$

Performing the same operations on equations (5) yields

$$\frac{Ch(3) - I(3) + \frac{B(3)}{A(3)} - L(3)}{S(3) - I(3)} = \frac{Ch(4) - I(4) + \frac{B(4)}{A(4)} - L(4)}{S(4) - I(4)} . \quad (7)$$

Equation (6) predicts a linear relationship between channel 1 and channel 2 while equation (7) also predicts a linear relationship for channel 3 and channel 4. Equation (7) is verified experimentally in both Figures 3 and 4. It is of interest to observe that the spread of data in these figures about the linear relationship is probably due to variation in S(i), I(i), and L(i) from one acquisition date to the other, but appears to have only a moderate effect on the linearity of the data.

If one solves equations (4) and (5) for e^{-n}, then the

relationship between channel i in the visible region (i=1,2) and channel j in the infrared (j=3,4) is

$$\left[\frac{Ch(i) - I(i) + \frac{B(i)}{A(i)} - L(i)}{S(i) - I(i)}\right]^{1/K_V} = \left[\frac{Ch(j) - I(j) + \frac{B(j)}{A(j)}}{S(j) - I(j)}\right]^{1/K_I} . \quad (8)$$

Equation (8) is a nonlinear relationship which has been observed experimentally in graphs of channel i versus channel j. This nonlinearity is due physically to differences in light attenuation through vegetative canopies that occur between visible and infrared wavelengths. For example, multitemporal plots of Landsat channel 2 versus channel 4 originate on the Kauth soil line, and as the crop grows and LAI increases channel 2 readings decrease and channel 4 readings increase. Channel 2 readings do not increase appreciably for LAI greater than 2 while channel 4 readings tend to increase up to LAI of 7, causing a vertical asymptote in the graph. In contrast, as has been seen from Figures 3 and 4, channel 3 versus channel 4 plots increase in a linear manner with detectable changes observed for LAI greater than 2 in both channels. Observations from Landsat data [21] further indicate that the visible channels are "noisy" and that there is a relatively small change in digital counts from bare soil radiance to infinite crop radiance which tends to compress the data on a small scale. It is for these reasons that the author selected plots of channel 3 versus channel 4 for analysis in this paper.

Use of Landsat Data to Determine LAI

Solving equation (5) for n in Landsat-1 (B(i)=0) gives

$$n = \frac{1}{K_I} \ell n \left[\frac{Ch(i) - I(i) - L(i)}{S(i) - I(i)} \right] \qquad (9)$$

which can be used for either channel 3 or channel 4. To demonstrate the use of equation (9), the sorghum data for channel 3 in Richardson [21] will be used to estimate LAI. The soil radiance for this data was unknown so the intersection of the regression line formed by the sorghum digital counts in channels 3 and 4 with the Kauth soils line was found, giving a value of 13. I(3) was calculated from the Richardson data for the digital count in channel 3 of the crop whose LAI is 8.5. Since L(3)=11 (see equations (3)), then

$$I(3) = 65 - 11 = 54.$$

Similarly, $S(3) = 13 - 11 = 2$.

The canopy extinction coefficient was calculated from data taken by LeMaster and Chance [20] for grain sorghum,

$$K_I = .49.$$

Equation (9) becomes

$$n = -2.04 \ell n \left[\frac{65 - Ch(3)}{52} \right] \qquad (10)$$

Table 3 is a comparison of the measured LAI for grain sorghum fields given by Richardson and the LAI values calculated by equation (10). The average error is an LAI of .66. The last three entries in Table 3 indicate that an infinite canopy reflectance occurs in channel 3 for an LAI between 5.1 and 6.9. Chance

and LeMaster [4] have used the vegetative canopy reflectance model developed by Suits [24] to calculate that infinite canopy reflectance occurs at an LAI of 6.11 in this wavelength region.

Conclusions

1. A method has been given to transform ground-based vegetative canopy reflectance data into the four Landsat MSS digital counts for a clear standard atmosphere. This transformation is simpler to apply than other known atmospheric models, and compares well with actual Landsat data.
2. Plots of Landsat channel 3 versus channel 4 multitemporal crop data yields information, both for crop discrimination and crop LAI.
3. Infinite crop reflectance spectra are important parameters that should be collected for vegetative canopies. This parameter may uniquely distinguish the different crops.
4. Crop LAI can be calculated for multitemporal Landsat data with prior knowledge of soil reflectance characteristics and crop infinite reflectance spectra.

REFERENCES

1. LeMaster, E. W., and Chance, J. E., "Further Tests of the Suits Reflectance Model," Proceedings of the Eleventh International Symposium on Remote Sensing of Environment, (1), 703, University of Michigan, Ann Arbor, April 1977.

2. Allen, W. A., and Richardson, A. J., "Interaction of light with a plant canopy," J. Opt. Soc. Am. 58, 219, (1968).

3. Hixson, M. H., Bauer, M. E., and Biehl, L. L., "Crop Spectra from LACIE Field Measurements," LARS-Purdue, Contract Report 011578, January 1978.

4. Chance, J. E., and LeMaster, E. W., "Suits reflectance models for wheat and cotton: theoretical and experimental tests," Appl. Opt. 16, 407 (1977).

5. Private Communications, Dr. Ross Leamer, 1978.

6. LeMaster, E. W., and Chance, J. E., "A seasonal verification of the Suits spectral reflectance model for wheat," to appear in Photogrammetric Engineering.

7. Norman, J. M., "Interfacing Leaf and Canopy Light Interception Model," Chapt V.C. in Predicting Photosynthate Production and Use for Ecosystem Models, CRC Press.

8. Turner, R. E., "Atmospheric Effects in Multispectral Remote Sensor Data," Report No. 109600-15-F, ERIM, Ann Arbor, Michigan, May 1975.

9. Elterman, L., "Atmospheric Attenuation Model, 1964, in the Ultraviolet, Visible, and Infrared Regions for Altitudes to 50 Km," Environmental Research Paper No. 46, (1964), Air Force Cambridge Research Laboratories, Office of Aerospace Research, United States Air Force, L. G. Hanscom Field, Mass.

10. Thekaekara, M. P., "The solar constant and spectral distribution of solar radiant flux," Solar Energy, 14, No. 2, 109-127.

11. Henderson, R. G., Thomas, G. S., and Nalepka, R. F., "Methods of Extending Signatures and Training without Ground Information," Report No. 109600-16-F, ERIM, Ann Arbor, Michigan, May 1975.

12. Richardson, A. J., Escobar, D. E., Gausman, H. W., and Everitt, J. H., "Comparison of Landsat-2 and Field Spectrometer Reflectance Signatures of South Texas Rangeland Plant Communities," Photogrammetric Eng. and Remote Sensing, submitted for publication.

13. Ahern, F. J., Goodenough, D. G., Jain, S. C., Rao, V. R., and Rochon, G., "Use of Clear Lakes as Standard Reflectors for Atmospheric Measurements," Proceedings of Eleventh International Symposium on Remote Sensing of Environment, I:731-755.

14. Private Communication, A. J. Richardson, June 25, 1979.

15. LeMaster, W. W., and Chance, J. E., Final Technical Report, "A Study of Bidirectional Reflectance Models for Plant Canopies and their Application to Biomass Determinations," NASA Contract NSG9033, 1978.

16. Gates, D. M., "Spectral distribution of solar radiation at the earth's surface," Science, 151, 532, 1966.

17. Condit, H. R., "The spectral reflectance of American soils," Photogrammetric Engr., Vol. 36, 955, 1970.

18. Kauth, R. J., and Thomas, G. S., "The Tasselled Cap--A Graphic Description of the Spectral-Temporal Development of Agricultural Crops as Seen by Landsat," Symp. Proc. Machine Processing of Remotely Sensed Data. LARS-Purdue IEEE Cat. 76 CH1103-01 MPRSD.

19. Richardson, A. J., and Wiegand, C. L., "Distinguishing vegetation from soil background information," Photogrammetric Engr. & Remote Sensing, Vol. 43, No. 12, 1541-1552, 1977.

20. LeMaster, E. W., and Chance, J. E., Final Technical Report, "Experimental and Theoretical Tests of a Modified Suits Model," NASA Contract NSG9033, 1979.

21. Richardson, A. J., Wiegand, C. L., Gausman, H. W., Cuellar, J. A., and Gerbermann, A. H., "Plant, soil and shadow reflectance components of row crops," Photogrammetric Engr. & Remote Sensing, Vol. 41 1401-1407, 1975.

22. Private Communcation, Dr. C. L. Wiegand, 1978.

23. Gausman, H. W., Allen, W. A., Wiegand, C. L., Escobar, D. E., Rodriques, R. R., and Richardson, A. J., "The Leaf Mesophylls of Twenty Crops, their Light Spectra, and Optical and Geometrical Parameters," Technical Bulletin No. 1465, United States Department of Agriculture, Washington, D.C., 1973.

24. Suits, G., "The calculation of the directional reflectance of a vegetative canopy," Remote Sensing of Environment 2, 197, 1972.

ACKNOWLEDGEMENTS

The author is indebted to NASA for funding this study under grant NSG 9033. A special debt of gratitude is due the staff at USDA-SEA Agricultural Research Service, Weslaco, Texas, for use of equipment, experimental test plots, sharing of data, and general support and encouragement. Dr. C. L. Wiegand, A. J. Richardson, Dr. Harold Gausman, and Dr. Ross Leamer were especially supportive of this author's efforts. My colleage, Dr. E. W. LeMaster, supplied many useful suggestions and comments, and Edith Hatfield gave the administrative support necessary to finish this project.

FIGURE CAPTIONS

Figure 1.

A comparison of bare soil reflectance for eastern Hidalgo County, Texas, with the infinite reflectance spectra for sugarcane and wheat.

Figure 2.

The Kauth soils line derived from equations (3) using data from Condit. The crosses are Landsat digital counts for bare soil taken from Richardson.

Figure 3.

A comparison of digital counts derived from equations (3) grain sorghum reflectance with Landsat digital counts for grain sorghum.

Figure 4.

A comparison of digital counts derived from equations (3) using wheat reflectance from two sites.

Figure 5.

Idealized multitemporal Landsat trajectories for four crops.

Channel	C(i)	D(i)	
1	.124	.637	1/22/75 to 7/15/75
2	1.342	5.983	
3	1.314	6.666	
4	1.146	2.197	
1	.970	3.980	7/16/75 to present
2	1.172	4.478	
3	1.200	5.217	
4	1.211	1.824	

Table 1.

Calibration Constants Required to Convert Equations (3) to Other Landsat Data. (Based on compiled calibration constants in [12])

Crop	Ch(1)	Ch(2)	Ch(3)	Ch(4)	Type of Data
Wheat	38	24	56	28	Landsat-1 simulation using equations (3) with a 28° solar zenith angle.
Grain sorghum	36	28	65	38	Landsat-1 data from Richardson [21] with 28° solar zenith angle.
Corn	29	22	67	33	Landsat-1 converted from Landsat-2 data by Table 1 with unknown solar zenith angle. Data supplied by Jerry Richardson, USDA-SEA, Weslaco, Texas.
Sugar-cane	43	33	81	34	Landsat-1 simulation using equations (3) from spectral reflectance data supplied by Dr. Ross Leamer, USDA-SEA, Weslaco, Texas.

Table 2.

Landsat-1 Digital Counts for Several Crops with Large LAI.

Channel 3 Landsat-1 Reading	Measured LAI	LAI from equation (10)
46	3.0	2.0
58	3.9	4.1
56	4.1	3.6
58	4.2	4.1
53	4.2	3.0
56	4.9	3.6
60	5.1	4.8
65	6.9	Undefined
67	7.3	Undefined
65	8.5	Undefined

Table 3.

A Comparison of LAI Calculated from equation (10) with Measured LAI Using Landsat-1 Data from Richardson for Ten Grain Sorghum Fields in a Single Frame.

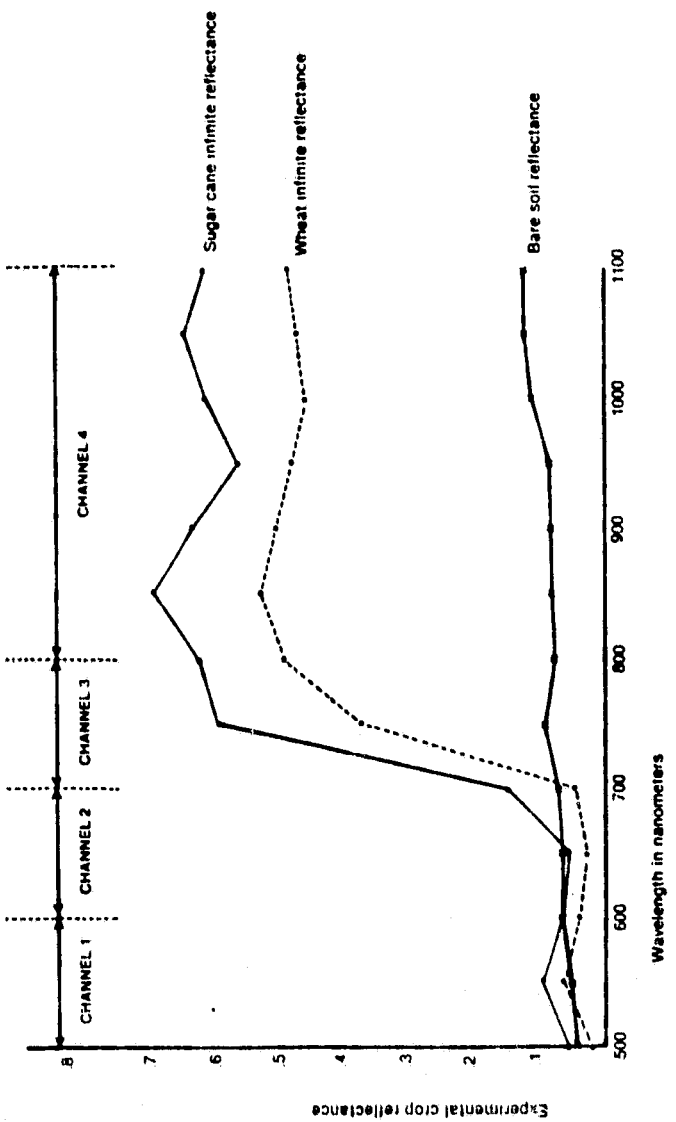

Figure 1

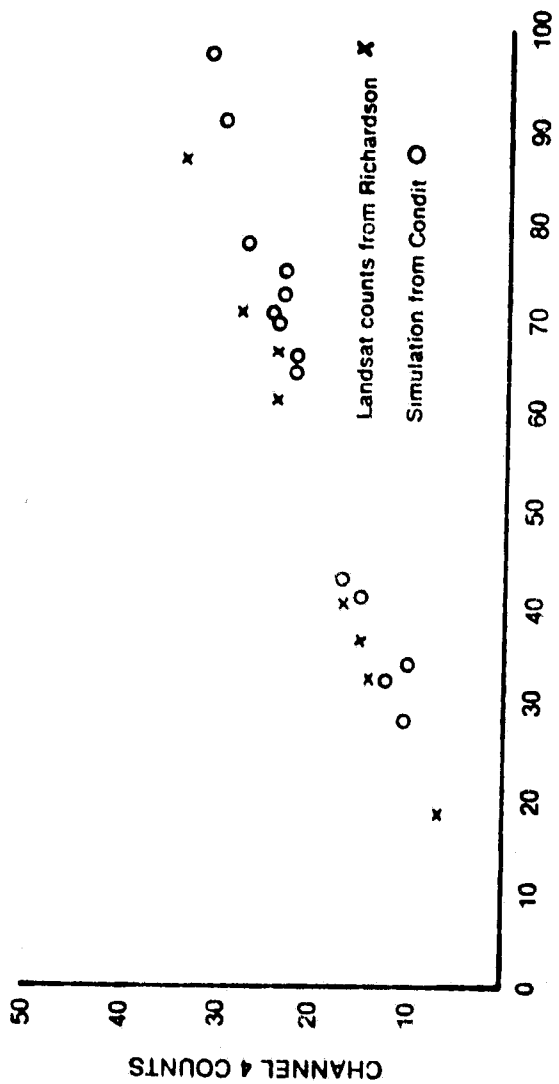

Figure 2

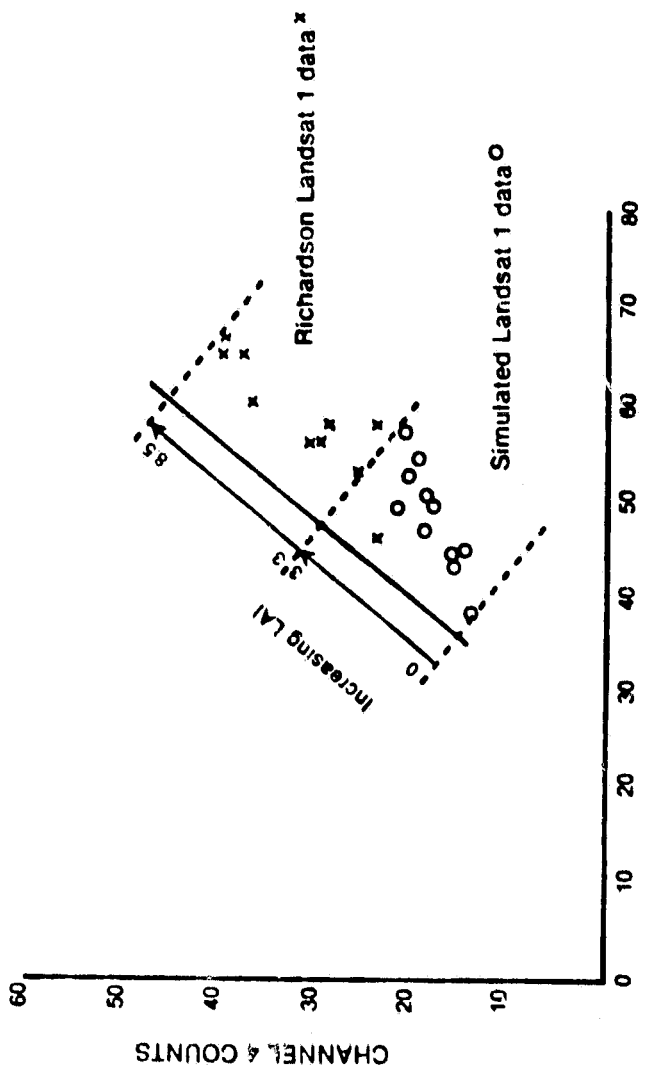

Figure 3

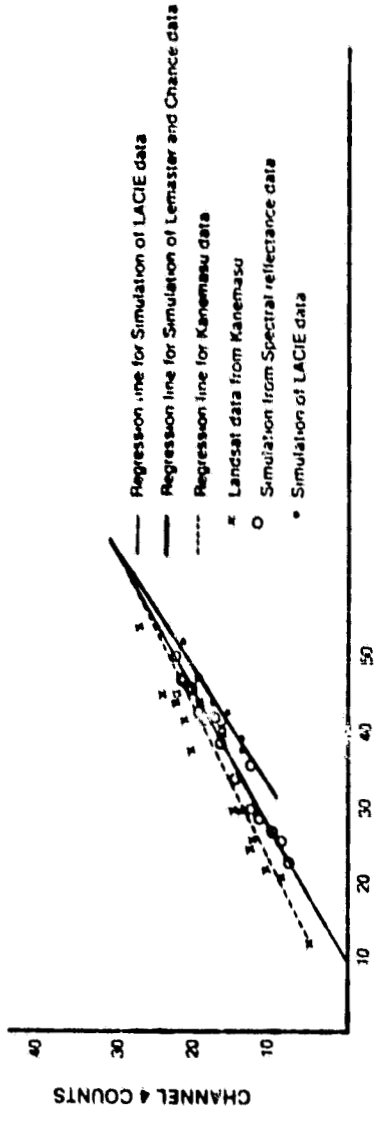

Figure 4

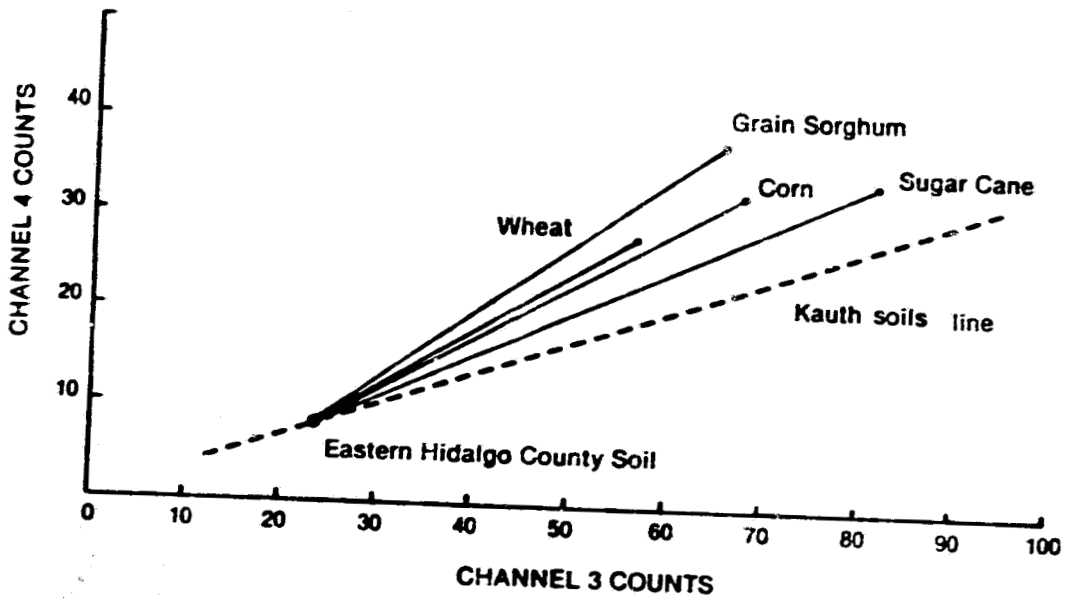

Figure 5